

97 **INTRODUCTION**

98

99 Urologic chronic pelvic pain syndrome (UCPPS) is an umbrella term encompassing
100 chronic visceral pain conditions, including interstitial cystitis/bladder pain syndrome
101 (IC/BPS). IC/BPS is a debilitating disorder affecting women predominantly and is
102 characterized by chronic pelvic pain and urinary frequency and urgency¹⁻⁷. IC/BPS is
103 also associated with anxiety and depression as well as gut microbiome alterations⁵.
104 Current treatment options for IC/BPS focus on symptoms and are non-curative,
105 reflecting an incomplete mechanistic understanding of disease pathogenesis and a lack
106 of validated biomarkers.

107 Neuroimaging studies from the MAPP Research Network have revealed changes
108 in white matter integrity and accelerated brain aging that correlate with pain severity⁸⁻¹⁰.
109 These findings indicate intrinsic CNS remodeling in IC/BPS and underscore the need to
110 identify specific biological pathways linking peripheral pathology to central pain
111 processing. An emerging hypothesis posits that initiating events in the bladder lead to
112 neuronal sensitization, which is subsequently amplified by immune-mediated
113 mechanisms involving central nervous system (CNS) immune cells, including microglia⁷.
114 However, the pathways linking peripheral pathology to central pain processing in
115 IC/BPS remain poorly defined.

116 Multiple studies in IC/BPS patients have reported gut dysbiosis, including
117 depletion of bacterial taxa involved in the biosynthesis of key metabolites known to
118 modulate gut health and gut-brain interactions^{5,11,12}. Preclinical models further support a
119 role for gut microbiota in IC/BPS pathophysiology, where mice lacking acyloxyacyl
120 hydrolase (AOAH) develop chronic pelvic pain resembling IC/BPS with associated gut
121 dysbiosis, where fecal transplant reduces pain^{13,14}. Notably, AOAH-deficient mice

122 display increased intestinal permeability and elevated circulating endotoxin levels,
123 which may cross the blood-brain barrier and activate immune CNS pathways¹³. To
124 evaluate the clinical relevance of such interactions, we examined responses of microglia
125 to patient stool microbiota. Microglia are macrophage-like CNS innate immune cells with
126 central roles in pain. Importantly, microglia express Toll-like receptors and receptors for
127 gut metabolites and thus are also transducers of gut-brain interactions. Here, we report
128 that stool microbiota of IC/BPS patients elicit stronger pro-inflammatory cytokine
129 responses in cultured microglia, relative to controls, and that cytokine responses correlate
130 with patient pain scores. These findings bolster a role for gut-brain interactions in
131 IC/BPS mediated by microglia and point to novel therapeutic opportunities.

132

133 **RESULTS**

134

135 **IC/BPS patients and healthy controls were recruited.** IC/BPS patients (n=16) and
136 healthy controls (n=16) were recruited through the Urology Clinic using established
137 inclusion and exclusion criteria⁵. IC/BPS participants were all female and exhibited
138 significantly higher GUPI pain, urinary, quality of life, and total scores compared to
139 controls (Table 1). Although the healthy control cohort was more racially diverse and
140 included a higher proportion of Black/ African American participants, race and ethnicity
141 were not significantly associated with disease status in this cohort (Table 1). However,
142 induced microglial cytokine responses did not differ among racial and ethnic groups of
143 control participants (Supplementary Figure 1), suggesting that any differences in
144 responses to patient and control microbiota were not influenced significantly by racial
145 and ethnic differences within the participant cohorts.

146

147 **IC/BPS stool microbiota elicit increased microglial proinflammatory cytokine**
148 **secretion.** We previously demonstrated that exposure of BV2 microglial cultures to heat-
149 killed stool slurry derived from IC/BPS patients induces higher expression of the
150 microglial activation marker CD68 compared to slurry from healthy controls, suggesting
151 that IC/BPS-associated microbiota can directly or indirectly activate microglia¹³. Here,
152 we extended these findings to assess cytokine and chemokine secretion in
153 complementary cell models using the mouse BV2 cell line, enriched primary cortical
154 murine microglia, and mixed cultures of primary cortical microglia and astrocytes to
155 mimic cell-cell interactions in the CNS. To validate the cellular composition and purity
156 of each *in vitro* system, immunofluorescence staining and flow cytometric analyses were

157 performed, confirming appropriate enrichment of microglial populations and astrocyte
158 representation in mixed glial cultures (Supplementary Figure 2). Primary microglia were
159 approximately 91% CD11b+, consistent with successful enrichment of microglia, whereas
160 mixed glial cultures were approximately 15% CD11b+, approximating the physiological
161 proportion of microglia in the murine brain. Initial multiplex cytokine profiling in
162 enriched primary microglia identified TNF- α , CCL5, and IL-6 as consistently responsive
163 inflammatory mediators among a broader panel of analytes, guiding focused
164 downstream analyses (Supplementary Figure 3).

165 Microglial cultures exposed to heat-killed stool slurry derived from IC/BPS
166 patients or healthy controls, and culture supernatants were evaluated by ELISA for TNF,
167 RANTES, and IL-6 (Figure 1). In BV2 microglial cultures, IC/BPS stool slurries elicited a
168 greater increase in tumor necrosis factor- α (TNF- α), CCL5/RANTES, and interleukin-6
169 (IL-6) secretion relative to healthy control microbiota (Figure 1A-C). Similar patterns
170 were observed in enriched primary microglia, where exposure to IC/BPS stool resulted
171 in significantly elevated TNF- α and CCL5 secretion, although IL-6 showed a more
172 modest and variable response (Figure 1D-F). In mixed glial cultures that incorporate
173 astrocyte-microglia interactions, IC/BPS stool induced significantly higher secretion of
174 TNF- α , CCL5, and IL-6 compared to healthy controls, with overall cytokine levels
175 exceeding those observed in microglia-only cultures (Figure 1G-I, compare to D-F).
176 Comparative analyses further demonstrated strong concordance in cytokine responses
177 between enriched microglia and mixed glial cultures following IC/BPS stool exposure,
178 supporting the robustness and reproducibility of these inflammatory signatures across in
179 vitro systems (Supplementary Figure 4).

180

181 **Microglial cytokine responses to IC/BPS microbiota correlate with patient-reported**
182 **pain.** To assess the clinical relevance of microbiome-induced glial activation, we next
183 examined whether cytokine responses correlated with patient-reported pain severity, as
184 measured by the Genitourinary Pain Index (GUPI). Across all *in vitro* systems, increased
185 cytokine secretion in response to IC/BPS stool microbiota was positively associated with
186 higher GUPI scores (Figure 2). In BV2 cultures, secretion of TNF- α , CCL5, and IL-6
187 demonstrated moderate to strong positive correlations with patient-reported pain
188 severity (Figure 2A–C). Similar relationships were observed in enriched primary
189 microglia, where TNF- α and CCL5 levels correlated significantly with GUPI scores, while
190 IL-6 showed a weaker, non-significant association (Figure 2D–F). In mixed glial cultures,
191 cytokine secretion exhibited the strongest correlations with pain severity, with TNF- α ,
192 CCL5, and IL-6 all demonstrating significant positive relationships with GUPI scores
193 (Figure 2G–I). Together, these findings link patient-derived IC/BPS microbiota to
194 microglial and glial inflammatory responses that scale with clinical pain severity,
195 supporting a translational association between gut dysbiosis, central immune activation,
196 and IC/BPS symptom burden.

197

198 **METHODS**

199

200 **Human subjects and stool sample collection.** Patient samples were collected under a
201 protocol approved by the Institutional Review Board. IC/BPS patients and healthy
202 controls were recruited through the Urology Clinic and enrolled using standard pelvic
203 pain inclusion and exclusion criteria, as previously described^{5,15}. Cohort demographics,
204 including race and ethnicity distribution, are summarized in Table 1. Because
205 Black/African American participants were overrepresented in the healthy control cohort,
206 we additionally examined cytokine distributions stratified by ethnicity (Supplementary
207 Figure 1).

208 Symptom severity was assessed using the Genitourinary Pain Index (GUPI)
209 questionnaire¹⁶ administered at the time of enrollment (Table 1). Stool samples were
210 collected according to approved protocols adapted from the Human Microbiome Project
211 Manual of Procedures, as previously described⁵. Briefly, participants collected stool
212 samples at home, froze them immediately, and shipped samples on wet ice. Upon receipt,
213 samples were aliquoted and stored at -80°C until further processing.

214 **Preparation of stool slurry.** Frozen stool samples were weighed and resuspended
215 in 1 mL Dulbecco's phosphate-buffered saline. Samples were vortexed, heat-inactivated
216 at 65°C for 15 min, filtered through a $0.22\ \mu\text{m}$ filter, and applied to cultures at a final
217 concentration of $1\ \mu\text{g}/\text{mL}$.

218 **Microglia culture models and stimulation.** Immortalized BV2 murine microglial
219 cells (AcceGen, Cat# ABC-TC212S) were maintained in Dulbecco's Modified Eagle
220 Medium supplemented with 10% fetal bovine serum (FBS) and 1% penicillin-
221 streptomycin. BV2 cells were plated at 1×10^5 cells/well, and on reaching confluency
222 were subsequently treated with stool slurry for 6 h prior to supernatant collection.

223 C57BL6/J mice were maintained on a 12hr:12hr light:dark cycle, and all
224 procedures were performed under an approved Institutional Animal Care and Use
225 Committee protocol. Primary mixed glial cultures (~80-90% astrocytes, ~10-20%
226 microglia) were prepared from postnatal day 0-2 mouse cortices. Briefly, cortices were
227 dissected, meninges removed, and tissue enzymatically dissociated using 0.25% trypsin
228 and 1 U/ μ L DNase I for 25 min at 37 °C. The resulting cell suspension was passed
229 through a 40 μ m cell strainer and plated in glial maintenance medium consisting of
230 DMEM supplemented with 10% FBS, 1% penicillin-streptomycin, and 2.5% GlutaMAX.
231 Mixed glial cultures were maintained until confluency and used for experiments between
232 days *in vitro* (DIV) 10–12. Cells were trypsinized and replated into 24-well plates at a
233 density of 1.4×10^6 cells per plate prior to treatment with stool slurry for 24 h.

234 Enriched microglial cultures were obtained using a modified shake-off protocol¹⁷.
235 Mixed glial cultures were grown to confluency until microglia were abundantly present
236 (DIV 13–15). Cultures were incubated with Versene (0.12 mM EDTA) at 37 °C for 2-3
237 min, followed by orbital shaking at 250 rpm for 3.5-4 h at 37 °C in fresh medium. The
238 supernatant containing detached microglia was collected, pelleted, and seeded at a
239 density of 0.5×10^5 cells per well onto poly-L-lysine coated 24-well plates. Enriched
240 microglia were maintained in glial maintenance medium supplemented with 10 ng/mL
241 recombinant murine macrophage colony-stimulating factor and treated with stool slurry
242 for 24 h.

243 **Cytokine measurements.** Cell culture supernatants were collected following
244 treatment and analyzed for cytokine secretion using enzyme-linked immunosorbent
245 assay (ELISA). Mouse TNF- α , CCL5/RANTES, and IL-6 DuoSet ELISA kits (R&D
246 Systems) were used according to the manufacturer's instructions. Cytokine
247 concentrations were calculated by four-parameter logistic curve fitting using GraphPad

248 Prism software. For multiplex cytokine profiling, the Mouse Cytokine Array C3
249 (RayBiotech) was used according to the manufacturer's protocol.

250 **Immunocytochemistry.** Immunofluorescence staining was performed on BV2
251 cells, enriched primary microglial, and mixed glial cultures. Briefly, cells were washed
252 with PBS and fixed in 4% paraformaldehyde (PFA, Sigma-Aldrich) for 20 min. After
253 washing, cells were permeabilized and blocked in PBS containing 0.2% bovine serum
254 albumin and 0.1% Triton X-100 for 60 min. Cultures were incubated overnight at 4 °C
255 with primary antibodies against mouse Iba1 (1:200; Cat# 019-19741, Fujifilm) and rabbit
256 GFAP (1:500; Cat# 3670S, Cell Signaling Technology). Following washes, cells were
257 incubated with appropriate fluorescent secondary antibodies (1:200, Invitrogen Life
258 Technologies) and DAPI (1:1000, Invitrogen Life Technologies) for 30 min at room
259 temperature. Images were acquired using a Nikon Ti2 widefield microscope (Nikon).

260 **Flow cytometry.** Cells were harvested, pelleted, and resuspended in anti-mouse
261 CD16/CD32 Fc blocking solution prior to staining. Samples were blocked on ice for 30
262 min and stained with fluorophore-conjugated antibodies against surface markers P2Y12
263 (anti-P2RY12 PE, Cat# 848003, BioLegend) and CD11b (anti-CD11b APC, Cat# 17-0112-81,
264 Invitrogen Life Sciences) for 1 h on ice. Cells were then fixed in 4% paraformaldehyde for
265 15 min, permeabilized, and stained for intracellular GFAP (anti-GFAP Alexa488, Cat# 53-
266 9892-82, Invitrogen Life Sciences). Samples were resuspended in PBS and analyzed on a
267 FACSymphony A5.2 spectral analyzer. Controls included unstained samples, single-
268 stained controls, and BV2 cells as microglial reference controls.

269 **Statistical analyses.** Data are presented as mean \pm SEM. Comparisons of cytokine
270 secretion between groups were performed using a two-tailed unpaired Student t-test.
271 Correlations between cytokine levels and GUPI scores were assessed using two-tailed
272 Pearson's correlation test. Normality was assessed using the Shapiro-Wilk test.

273 Statistical analyses were conducted using GraphPad Prism (version 10), and $p < 0.05$ was
274 considered statistically significant.

275

276 **DISCUSSION**

277

278 IC/BPS is characterized by heterogeneous clinical presentations and poorly
279 defined etiologies, complicating diagnosis, clinical management, and therapeutic
280 development. Identifying convergent biological pathways that link peripheral pathology
281 to central pain processing is a critical unmet need. We previously reported that exposure
282 of BV2 microglia to IC/BPS-associated fecal microbiota induces greater activation
283 compared to healthy control microbiota, as assessed by increased CD68 expression¹³.
284 Here, we extend those findings by demonstrating enhanced secretion of proinflammatory
285 cytokines TNF- α , IL-6, and RANTES/CCL5, in response to patient-derived IC/BPS
286 microbiota (Figure 1). This effect is consistent across immortalized BV2 cells, enriched
287 primary microglia, and mixed glial cultures. Importantly, the cytokine secretion
288 positively correlates with patient-reported pain severity, as measured by the GUPI scores
289 (Figure 2). Together, these findings position microglia as a mechanistic node linking gut
290 dysbiosis to CNS immune activation in IC/BPS.

291 Microglia are central regulators of neuronal excitability and synaptic plasticity
292 during chronic pain states¹⁸. Prior studies demonstrate that microglial activation
293 contributes to central sensitization through the release of proinflammatory mediators and
294 chemokines, which can directly influence neuronal signaling and glial-neuronal
295 interactions^{19,20}. Microglia also express Toll-like receptors and nuclear receptors for
296 hydrophobic ligands and thus are poised to respond to circulating products of gut
297 microbiota including microbial structural components and metabolites⁷. Consistent with
298 this literature, we observed robust induction of TNF- α , IL-6 and RANTES/CCL5 in
299 response to IC/BPS-associated microbiota across *in vitro* microglial models.

300 The distinct behavior of IL-6 relative to TNF- α and RANTES in enriched primary
301 microglial cultures likely reflects differences in cytokine regulation and cellular context.
302 IL-6 signaling in the CNS is known to be highly modulatory and is often refined or
303 amplified through astrocyte–microglia interactions, whereas TNF- α and chemokines
304 such as RANTES are rapidly induced as part of early microglia-intrinsic innate
305 responses²¹. Although microglia appear sufficient to mount inflammatory responses to
306 IC/BPS-associated microbiota, our data also highlight the importance of glial crosstalk in
307 shaping CNS inflammation. Mixed glial cultures, which incorporate astrocytes alongside
308 microglia, exhibited amplified cytokine responses compared to enriched microglial
309 cultures, consistent with the known role of astrocytes in propagating and sustaining
310 inflammatory signaling²². At the same time, the strong correlation of cytokine responses
311 between enriched microglia and mixed glia supports the use of both systems as
312 complementary and translationally relevant *in vitro* models.

313 We have previously shown that pharmacological ablation of microglia using the
314 CSF1R inhibitor PLX5622 attenuates pelvic allodynia in the IC/BPS model of AOA-H-
315 deficient mice, supporting a functional role for microglia in pain amplification¹³.
316 Similarly, minocycline suppresses microglial activation and has been shown to reduce
317 neuroinflammatory signaling and pain-related outcomes in preclinical and clinical
318 studies^{23,24}. Together, these observations reinforce the therapeutic relevance of targeting
319 microglial activation in chronic pain states, including IC/BPS.

320 Patients with IC/BPS consistently exhibit gut dysbiosis, and symptoms are
321 frequently exacerbated by dietary triggers, supporting a role for gut-derived signaling in
322 pain manifestation⁷. Alterations in fecal microbiota have also been reported in chronic
323 prostatitis/chronic pelvic pain syndrome, suggesting that microbiome-driven
324 mechanisms may extend across UCPPS phenotypes^{7,25}.

325 Accumulating evidence supports a critical role for bidirectional communication
326 between the gut microbiota and the CNS in the pathophysiology of chronic pain, anxiety
327 and depression, and neurodegenerative diseases^{26,27}. In IC/BPS, patients exhibit gut
328 dysbiosis, and symptoms are commonly exacerbated by comestibles including acidic
329 foods and caffeine^{28,29}, supporting a role for gut-derived signaling in pain manifestation
330 (reviewed in ⁷). Notably, neuroimaging studies from the Multidisciplinary Approach to
331 the Study of Chronic Pelvic Pain (MAPP) Research Network have identified CNS
332 alterations in IC/BPS patients, including changes in white matter microstructure and
333 accelerated brain aging that correlate with pain severity, particularly in women.
334 Although these imaging studies do not directly resolve specific glial populations, white
335 matter alterations and signatures of neuroinflammation are increasingly recognized as
336 reflecting glial dysfunction. Similar imaging patterns suggestive of neuroinflammation
337 have been described across chronic pain conditions, supporting a broader role for glial-
338 mediated CNS remodeling in persistent pain states³⁰. Our data begin to bridge this gap
339 by providing a biological pathway through which peripheral dysbiosis may engage CNS
340 immune mechanisms, specifically microglial activation, to influence pain processing.

341 Collectively, these data support a model in which IC/BPS-associated gut dysbiosis
342 promotes microglial activation, potentially leading to central sensitization and pain
343 amplification. Restoration of microbial homeostasis therefore represents a promising
344 therapeutic strategy. Prior work demonstrating that correction of dysbiosis through fecal
345 microbiota transfer or co-housing alleviates pelvic pain in preclinical models supports
346 the concept that upstream microbial signals are modifiable contributors to CNS
347 dysfunction. Future studies integrating microbiome, metabolomic, and neuroimaging
348 approaches will be critical to determine whether microbiome-targeted interventions,

349 including probiotics or defined microbial consortia, can attenuate microglial activation
350 and reduce pelvic pain in IC/BPS and related UCPPS conditions.
351

353 REFERENCES

354

- 355 1 Partin AW, Wein AJ, Kavoussi LR, Peters CA, Dmochowski RR. *Campbell-Walsh-Wein*
 356 *Urology Twelfth Edition Review*. 12th edn. 2020.
- 357 2 Griffith JW, Stephens-Shields AJ, Hou X, Naliboff BD, Pontari M, Edwards TC, *et al.*
 358 Pain and Urinary Symptoms Should Not be Combined into a Single Score:
 359 Psychometric Findings from the MAPP Research Network. *J Urol* 2016;**195**:949–54.
 360 <https://doi.org/10.1016/j.juro.2015.11.012>.
- 361 3 Hanno PM, Erickson D, Moldwin R, Faraday MM, American Urological Association.
 362 Diagnosis and treatment of interstitial cystitis/bladder pain syndrome: AUA
 363 guideline amendment. *J Urol* 2015;**193**:1545–53.
 364 <https://doi.org/10.1016/j.juro.2015.01.086>.
- 365 4 Clemens JQ, Mullins C, Ackerman AL, Bavendam T, van Bokhoven A, Ellingson BM,
 366 *et al.* Urologic chronic pelvic pain syndrome: insights from the MAPP Research
 367 Network. *Nat Rev Urol* 2019;**16**:187–200. <https://doi.org/10.1038/s41585-018-0135-5>.
- 368 5 Braundmeier-Fleming A, Russell NT, Yang W, Nas MY, Yaggie RE, Berry M, *et al.*
 369 Stool-based biomarkers of interstitial cystitis/bladder pain syndrome. *Sci Rep*
 370 2016;**6**:26083. <https://doi.org/10.1038/srep26083>.
- 371 6 Mullins C, Bavendam T, Kirkali Z, Kusek JW. Novel research approaches for
 372 interstitial cystitis/bladder pain syndrome: thinking beyond the bladder. *Transl*
 373 *Androl Urol* 2015;**4**:524–33. <https://doi.org/10.3978/j.issn.2223-4683.2015.08.01>.
- 374 7 Klumpp DJ. Microbiota in interstitial cystitis/bladder pain syndrome: evidence and
 375 opportunities. *J Clin Invest* n.d.;**135**:e197858. <https://doi.org/10.1172/JCI197858>.
- 376 8 Wang C, Kutch JJ, Labus JS, Yang CC, Harris RE, Mayer EA, *et al.* Reproducible
 377 Microstructural Changes in the Brain Associated With the Presence and Severity of
 378 Urologic Chronic Pelvic Pain Syndrome (UCPPS): A 3-Year Longitudinal Diffusion
 379 Tensor Imaging Study From the MAPP Network. *J Pain* 2023;**24**:627–42.
 380 <https://doi.org/10.1016/j.jpain.2022.11.008>.
- 381 9 Leech KA, Kettlety SA, Mack WJ, Kreder KJ, Schrepf A, Kutch JJ. Brain predicted age
 382 in chronic pelvic pain: a study by the Multidisciplinary Approach to the Study of
 383 Chronic Pelvic Pain Research Network. *Pain* 2025;**166**:1060–9.
 384 <https://doi.org/10.1097/j.pain.0000000000003424>.
- 385 10Huang L, Kutch JJ, Ellingson BM, Martucci KT, Harris RE, Clauw DJ, *et al.* Brain
 386 white matter changes associated with urological chronic pelvic pain syndrome:
 387 multisite neuroimaging from a MAPP case-control study. *Pain* 2016;**157**:2782–91.
 388 <https://doi.org/10.1097/j.pain.0000000000000703>.
- 389 11Jiang P, Li C, Su Z, Chen D, Li H, Chen J, *et al.* Mendelian randomization study
 390 reveals causal effects of specific gut microbiota on the risk of interstitial
 391 cystitis/bladder pain syndrome (IC/BPS). *Sci Rep* 2024;**14**:18405.
 392 <https://doi.org/10.1038/s41598-024-69543-9>.
- 393 12Fu C, Zhao Y, Zhou X, Lv J, Jin S, Zhou Y, *et al.* Gut microbiota and interstitial cystitis:
 394 exploring the gut-bladder axis through mendelian randomization, biological
 395 annotation and bulk RNA sequencing. *Front Immunol* 2024;**15**:1395580.
 396 <https://doi.org/10.3389/fimmu.2024.1395580>.
- 397 13Rahman-Enyart A, Yaggie RE, Bollinger JL, Arvanitis C, Winter DR, Schaeffer AJ, *et*
 398 *al.* Acyloxyacyl hydrolase regulates microglia-mediated pelvic pain. *PLoS One*
 399 2022;**17**:e0269140. <https://doi.org/10.1371/journal.pone.0269140>.

- 400 14 Yang W, Yaggie RE, Jiang MC, Rudick CN, Done J, Heckman CJ, *et al.* Acyloxyacyl
401 hydrolase modulates pelvic pain severity. *Am J Physiol Regul Integr Comp Physiol*
402 2018;**314**:R353–65. <https://doi.org/10.1152/ajpregu.00239.2017>.
- 403 15 Landis JR, Williams DA, Lucia MS, Clauw DJ, Naliboff BD, Robinson NA, *et al.* The
404 MAPP research network: design, patient characterization and operations. *BMC Urol*
405 2014;**14**:58. <https://doi.org/10.1186/1471-2490-14-58>.
- 406 16 Clemens JQ, Calhoun EA, Litwin MS, McNaughton-Collins M, Kusek JW, Crowley
407 EM, *et al.* Validation of a modified National Institutes of Health chronic prostatitis
408 symptom index to assess genitourinary pain in both men and women. *Urology*
409 2009;**74**:983–7, quiz 987.e1-3. <https://doi.org/10.1016/j.urology.2009.06.078>.
- 410 17 Daniele SG, Edwards AA, Maguire-Zeiss KA. Isolation of cortical microglia with
411 preserved immunophenotype and functionality from murine neonates. *J Vis Exp*
412 2014:e51005. <https://doi.org/10.3791/51005>.
- 413 18 Ji D, Lyu Z, Erasmus S, Wu Y, Li X, Chen X, *et al.* Microglia's Phenotypic
414 Heterogeneity in Pain Pathogenesis and Electroacupuncture Analgesia: Mechanisms
415 and Therapeutic Potential. *J Pain Res* 2025;**18**:6007–22.
416 <https://doi.org/10.2147/JPR.S545420>.
- 417 19 Chen G, Zhang Y-Q, Qadri YJ, Serhan CN, Ji R-R. Microglia in Pain: Detrimental and
418 protective roles in pathogenesis and resolution of pain. *Neuron* 2018;**100**:1292–311.
419 <https://doi.org/10.1016/j.neuron.2018.11.009>.
- 420 20 Inoue K, Tsuda M. Microglia in neuropathic pain: cellular and molecular mechanisms
421 and therapeutic potential. *Nat Rev Neurosci* 2018;**19**:138–52.
422 <https://doi.org/10.1038/nrn.2018.2>.
- 423 21 Gruol DL. IL-6 regulation of synaptic function in the CNS. *Neuropharmacology*
424 2015;**96**:42–54. <https://doi.org/10.1016/j.neuropharm.2014.10.023>.
- 425 22 Liddel SA, Barres BA. Reactive Astrocytes: Production, Function, and Therapeutic
426 Potential. *Immunity* 2017;**46**:957–67. <https://doi.org/10.1016/j.immuni.2017.06.006>.
- 427 23 Liu C-C, Lu N, Cui Y, Yang T, Zhao Z-Q, Xin W-J, *et al.* Prevention of Paclitaxel-
428 induced allodynia by Minocycline: Effect on loss of peripheral nerve fibers and
429 infiltration of macrophages in rats. *Mol Pain* 2010;**6**:76. <https://doi.org/10.1186/1744-8069-6-76>.
- 430 24 Syngle A, Verma I, Krishan P, Garg N, Syngle V. Minocycline improves peripheral
431 and autonomic neuropathy in type 2 diabetes: MIND study. *Neurol Sci* 2014;**35**:1067–
432 73. <https://doi.org/10.1007/s10072-014-1647-2>.
- 433 25 Shoskes DA, Wang H, Polackwich AS, Tucky B, Altemus J, Eng C. Analysis of Gut
434 Microbiome Reveals Significant Differences between Men with Chronic
435 Prostatitis/Chronic Pelvic Pain Syndrome and Controls. *J Urol* 2016;**196**:435–41.
436 <https://doi.org/10.1016/j.juro.2016.02.2959>.
- 437 26 Meerschaert KA, Chiu IM. The gut–brain axis and pain signalling mechanisms in the
438 gastrointestinal tract. *Nat Rev Gastroenterol Hepatol* 2025;**22**:206–21.
439 <https://doi.org/10.1038/s41575-024-01017-9>.
- 440 27 Ho T, Elma Ö, Kocanda L, Brain K, Lam T, Kanhere T, *et al.* The brain-gut axis and
441 chronic pain: mechanisms and therapeutic opportunities. *Front Neurosci*
442 2025;**19**:1545997. <https://doi.org/10.3389/fnins.2025.1545997>.
- 443 28 Shorter B, Lesser M, Moldwin RM, Kushner L. Effect of comestibles on symptoms of
444 interstitial cystitis. *J Urol* 2007;**178**:145–52. <https://doi.org/10.1016/j.juro.2007.03.020>.
- 445 29 Alagiri M, Chottiner S, Ratner V, Slade D, Hanno PM. Interstitial cystitis:
446 unexplained associations with other chronic disease and pain syndromes. *Urology*
447 1997;**49**:52–7. [https://doi.org/10.1016/s0090-4295\(99\)80332-x](https://doi.org/10.1016/s0090-4295(99)80332-x).
- 448

449 30Loggia ML. “Neuroinflammation”: does it have a role in chronic pain? Evidence from
450 human imaging. *Pain* 2024;**165**:S58–67.
451 <https://doi.org/10.1097/j.pain.0000000000003342>.
452
453

454 **FIGURE LEGENDS**

455

456 **Figure 1. IC/BPS stool microbiota elicit increased proinflammatory cytokine secretion**
457 **across microglial culture systems.** BV2 cells (a–c), enriched primary microglia (d–f), and
458 mixed glial cultures (g–i) were treated with 1 $\mu\text{g}/\text{mL}$ heat-killed stool slurry derived from
459 healthy controls (HC) or IC/BPS patients (IC). After stimulation, concentrations of TNF-
460 α (a, d, g), RANTES (b, e, h), and IL-6 (c, f, i) in culture supernatants were quantified by
461 ELISA. Data are presented as mean \pm SEM, with individual data points representing
462 independent patient stool samples. Statistical comparisons between HC and IC groups
463 were performed using two-tailed unpaired Student's t-tests. $p < 0.05$ indicates statistical
464 significance.

465

466 **Figure 2. Microglial cytokine responses to IC/BPS stool microbiota correlate with**
467 **patient-reported pain severity.** Cytokine levels secreted by BV2 microglial cell line (a–c),
468 enriched primary microglia (d–f), and mixed glial cultures (g–i) in response to patient-
469 derived stool slurry were plotted against the corresponding total Genitourinary Pain
470 Index (GUPI) score of the same patient. TNF- α (a, d, g), RANTES (b, e, h), and IL-6 (c, f,
471 i) concentrations were quantified by ELISA. Correlations were assessed using two-tailed
472 Pearson's correlation analysis; correlation coefficients (r) and p values are shown in each
473 panel. Solid lines indicate linear regression fits with dashed lines representing 95%
474 confidence intervals.

475 **Table 1. Clinical cohort characterization of IC/BPS and healthy control donors.**

476

	Healthy controls	IC/BPS patients	p-value
Age	36.31 ± 14.1	41.56 ± 15	0.317
Sex (F, %)	0.00	100.00	0.0028
Genitourinary Pain Index (GUPI)			
GUPI - Pain	56.25	11.94 ± 3.9	<0.0001
GUPI - Urinary	0.25 ± 0.4	4.25 ± 1.9	<0.0001
GUPI - QOL	0.12 ± 0.3	7.44 ± 3.2	<0.0001
GUPI - total	0.37 ± 0.5	23.69 ± 7.5	<0.0001
Ethnicity, n (%)			
Asian/Asian American	1 (6%)	0 (0%)	0.281
Black/African American	7 (44%)	3 (19%)	
Hispanic/Latino	1 (6%)	2 (13%)	
White	7 (44%)	11 (69%)	

477

Figure 1. IC/BPS stool microbiota elicit increased proinflammatory cytokine secretion across microglial culture systems.

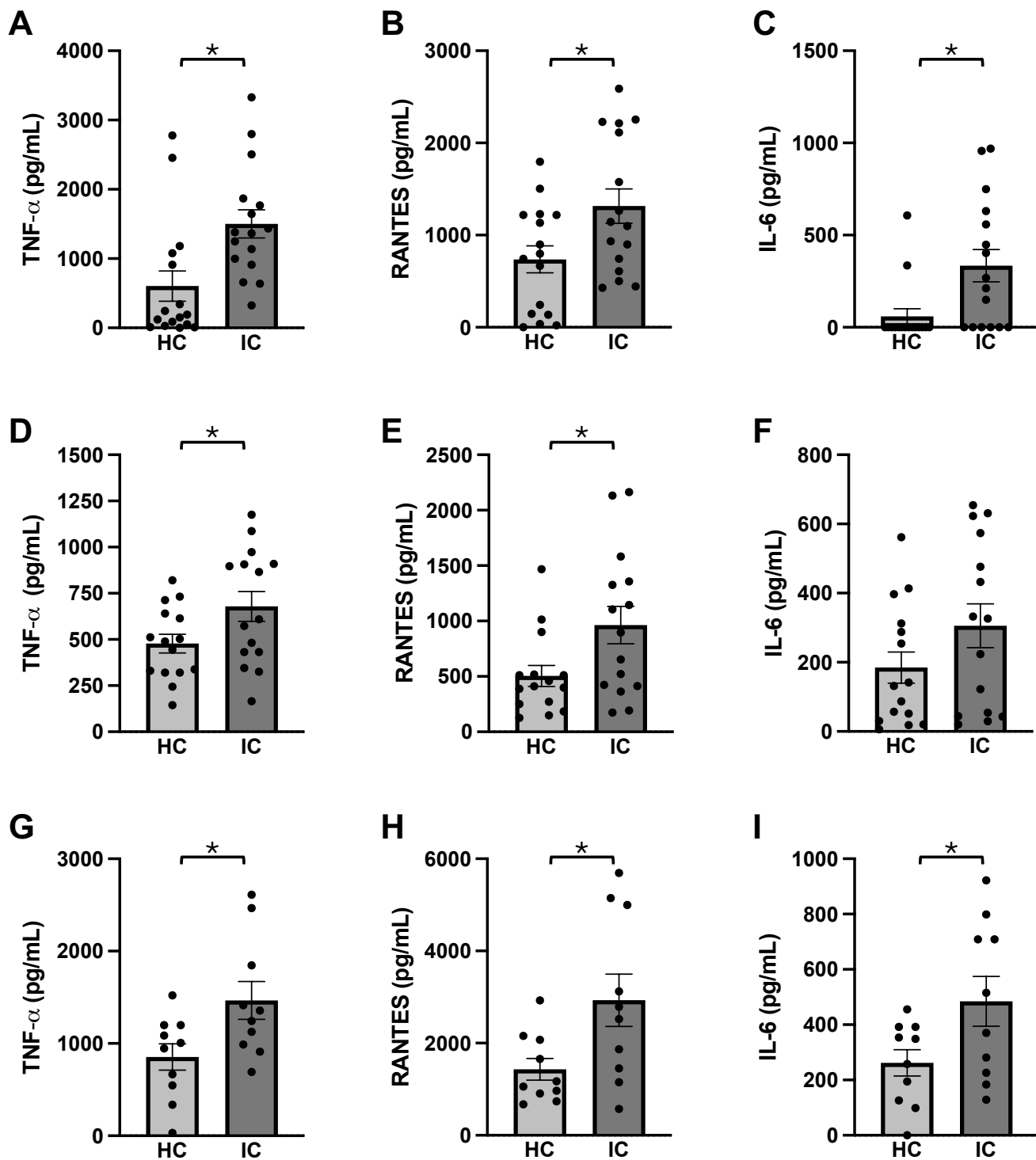
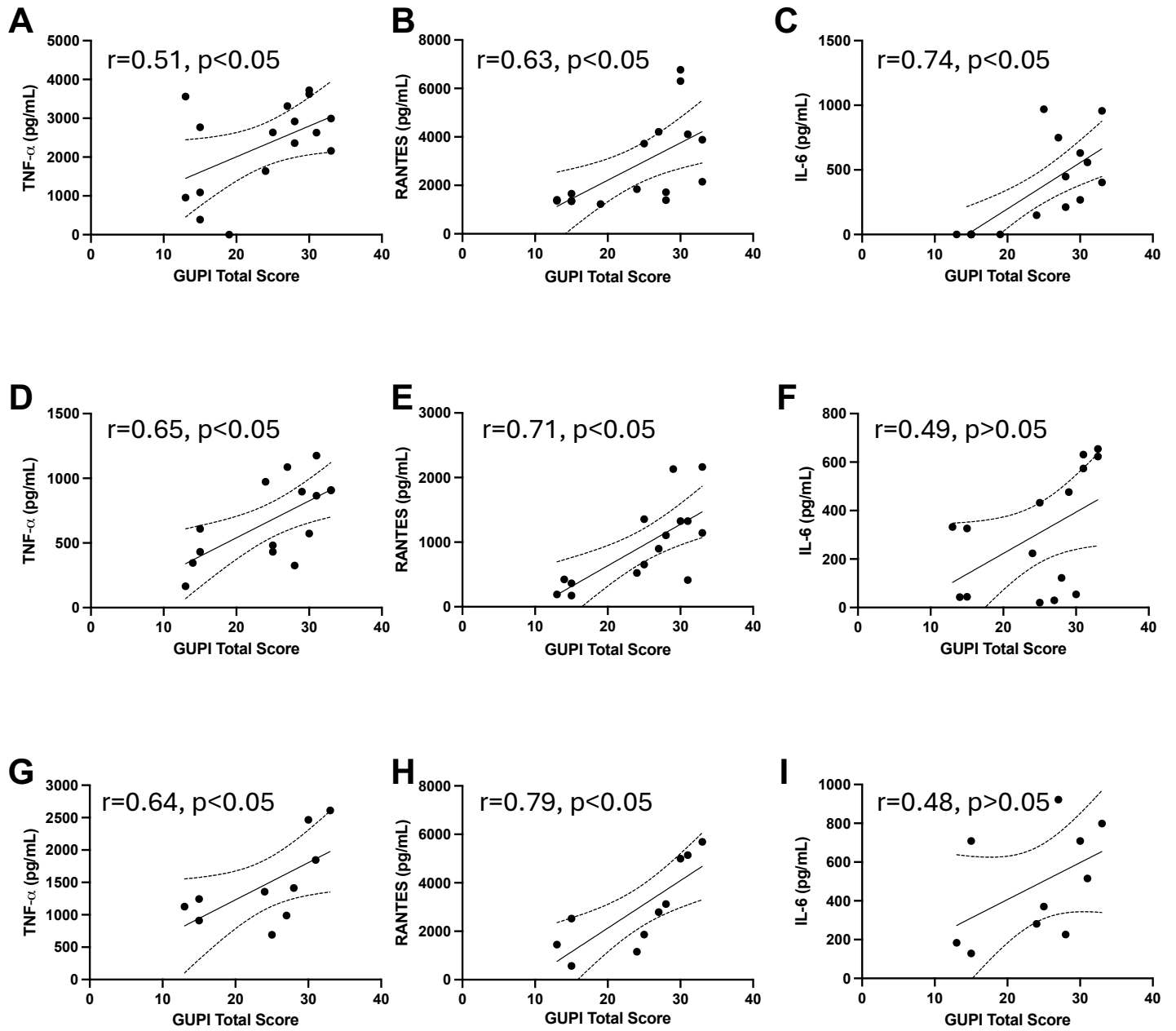


Figure 2. Microglial cytokine responses to IC/BPS stool microbiota correlate with patient-reported pain severity.



478 **SUPPLEMENTARY DATA**

479

480 **Supplementary Figure 1. Distribution of microglial cytokine secretion by ethnicity**

481 **among healthy control donors.** Cytokine secretion in response to stool slurry derived
482 from healthy control donors was stratified by donor's ethnicity. BV2 microglial cell line
483 responses are shown in panels (A–C), enriched primary microglia in panels (D–F), and
484 mixed glial cultures in panels (G–I). TNF- α (A, D, G), RANTES/CCL5 (B, E, H), and IL-6
485 (C, F, I) concentrations were quantified by ELISA following treatment with 1 μ g/mL heat-
486 killed stool slurry. Bars represent mean \pm SEM, with individual data points corresponding
487 to independent healthy control stool donors. No significant differences in cytokine
488 secretion were observed across racial/ethnic groups within the healthy control cohort
489 (one-way ANOVA or Kruskal–Wallis test, as appropriate; $p > 0.05$).

490

491 **Supplementary Figure 2. Validation of *in vitro* models by immunofluorescence and**

492 **flow cytometry.** Immunofluorescence staining with Iba1 (green), GFAP (red) and DAPI

493 (blue) was performed on (a) BV2 cells, (b) enriched primary microglia, and (c) mixed glial

494 cultures. *In vitro* models were further validated using flow cytometry using CD11b, F4/80

495 and P2Y12 microglial markers, and GFAP as astrocytic marker. Representative plots in

496 (d) show unstained (negative control, left) and BV2 (right) samples, with 94.7% CD11b+

497 F4/80+ and 98.4% CD11b+ P2Y12+ cells. Panel (e) shows 91.3% CD11b+ F4/80+ and

498 94.6% CD11b+ P2Y12+, while panel (f) shows 66% GFAP+ and 14.8% CD11b+ P2Y12+

499

500 **Supplementary Figure 3. Multiplex cytokine profiling in enriched primary microglia**

501 **identifies key inflammatory readouts among 62 analytes.** Supernatants from enriched

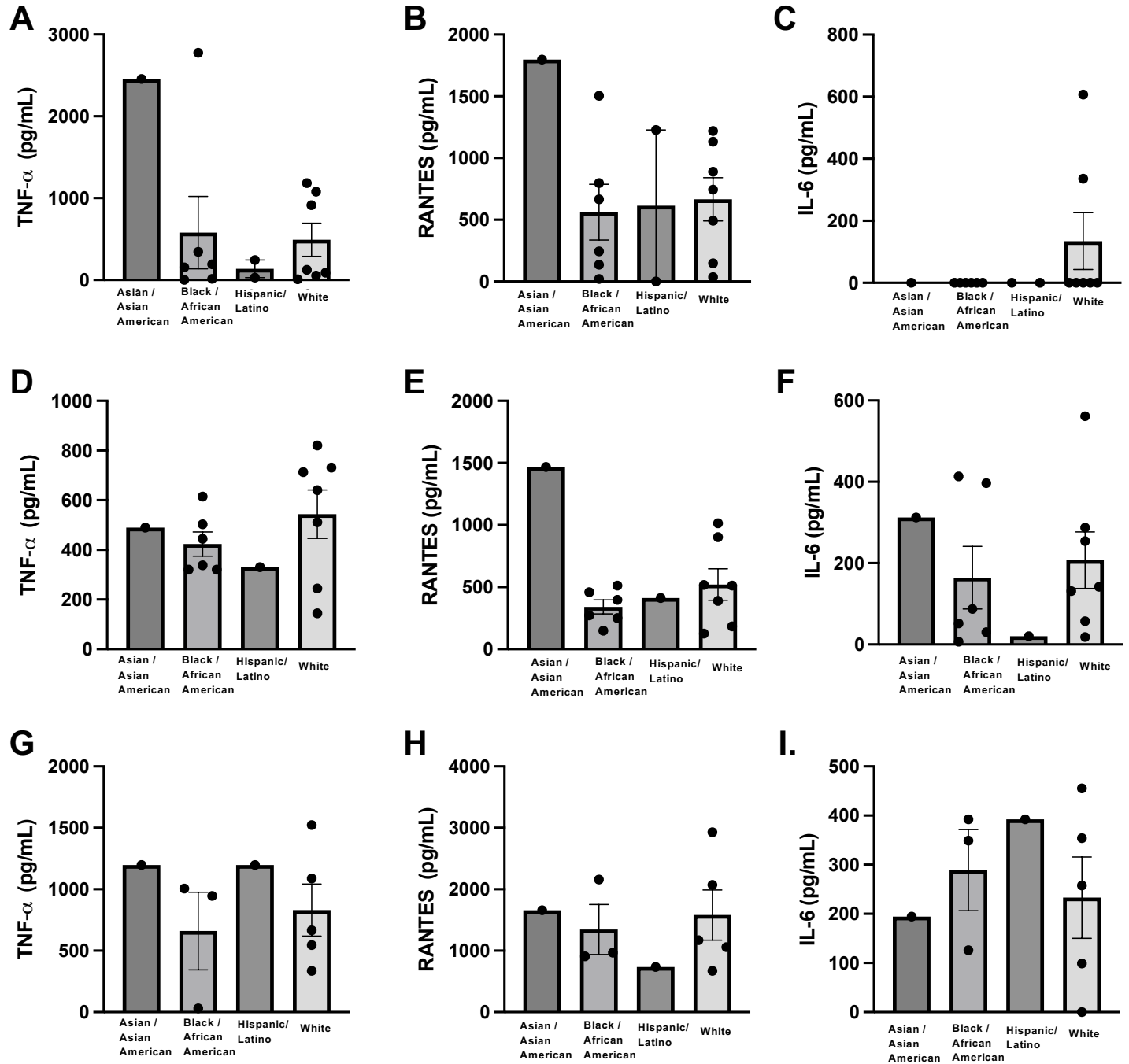
502 microglia were analyzed for potential cytokine and chemokine secretion in response to

503 stool slurry from healthy controls (HC) or IC patients (IC), as well as control treatments
504 including untreated, LPS and IL-4 conditions. (a) Representative composite image
505 showing chemiluminescent detection from eight cytokine array membranes analyzed
506 simultaneously. (b) Heatmap of normalized cytokine levels averaged across HC and IC
507 groups, highlighting differential expression of inflammatory mediators.

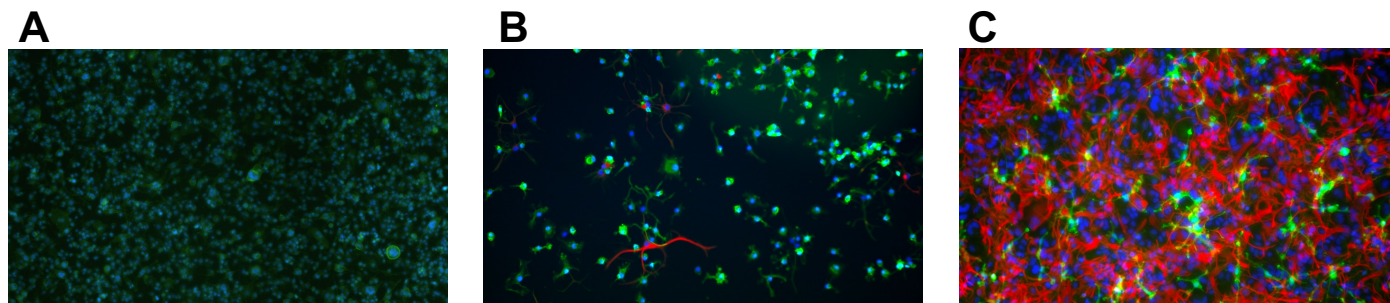
508

509 **Supplementary Figure 4. Comparison of cytokine responses between enriched**
510 **microglia and mixed glia reveals shared trends.** Cytokine secreted from enriched
511 microglia and mixed glia in response to stool slurry from IC/BPS patients were plotted
512 against each other to compare the two responses between the two in vitro models. Strong
513 positive correlations were observed between cytokine levels across models for (a) TNF-
514 α , (b) RANTES, and (c) IL-6. Statistical analysis performed using a two-tailed Pearson's
515 correlation; $p < 0.05$ was considered significant.

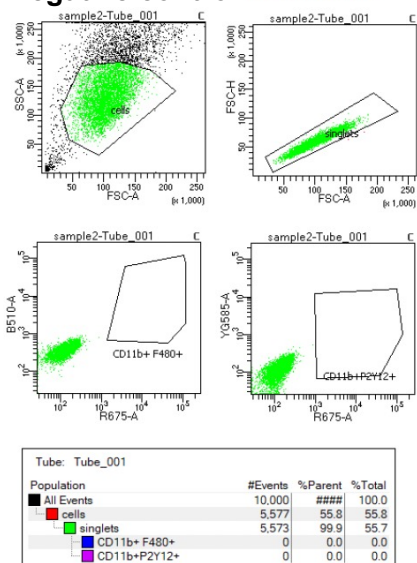
Supplement Fig 1. Distribution of microglial cytokine secretion by ethnicity among healthy control donors



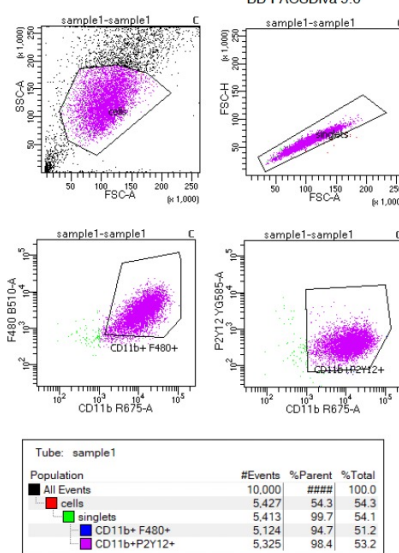
Supplement Fig 2. Validation of in vitro models by immunofluorescence and flow cytometry.



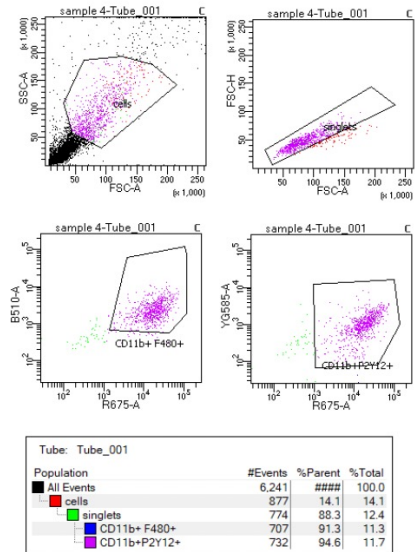
D Negative control BD FACSDiva 9.6



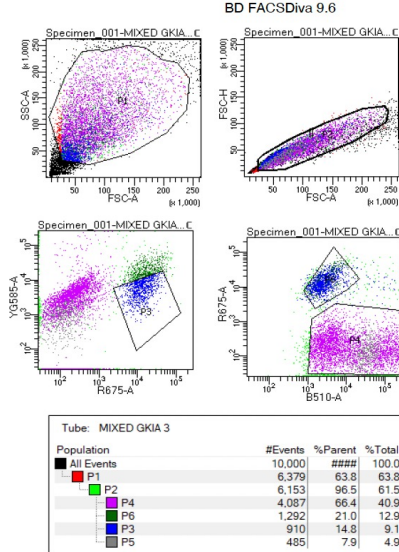
BD FACSDiva 9.6



E BD FACSDiva 9.6

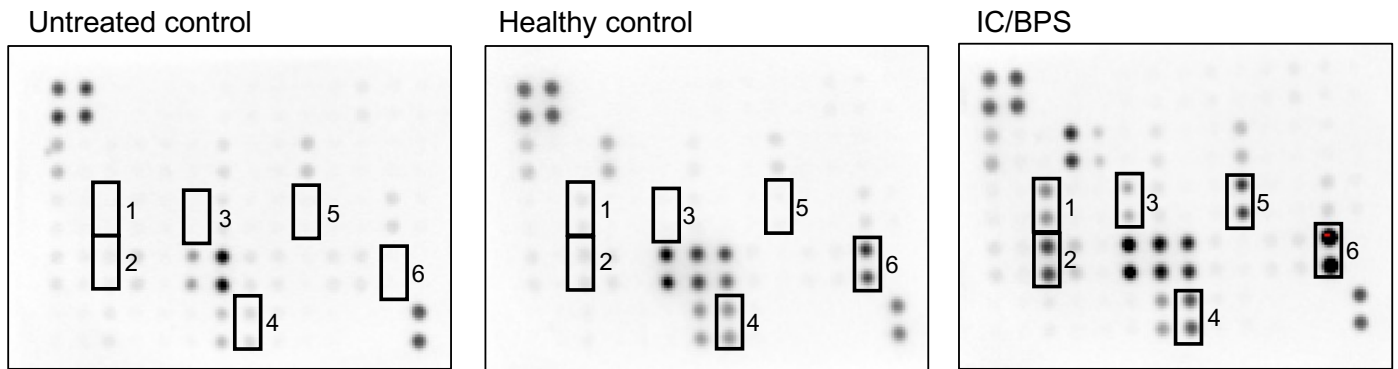


F BD FACSDiva 9.6



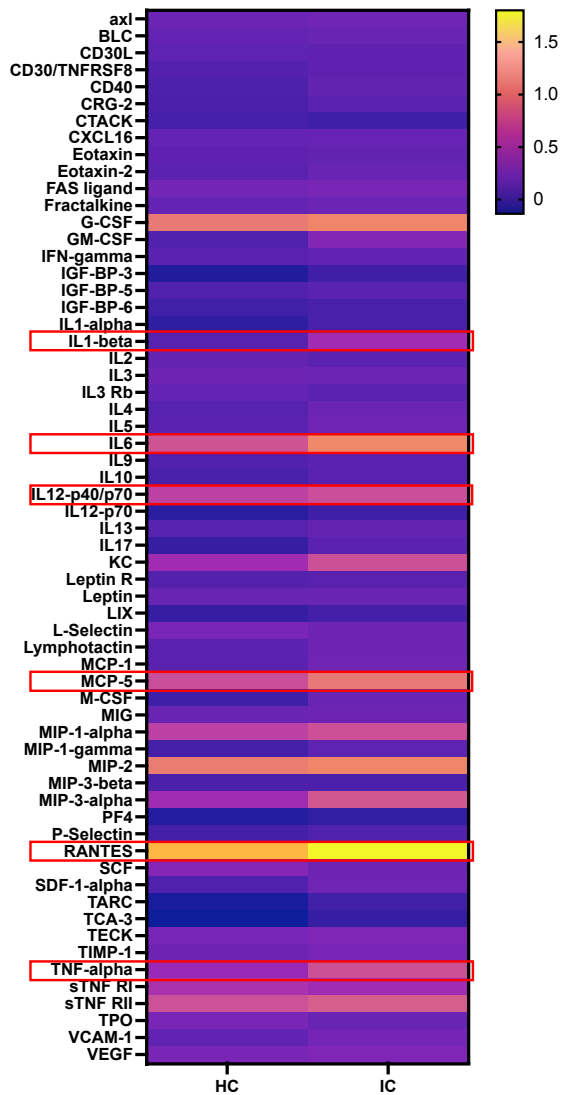
Supplement Fig 3. Multiplex cytokine profiling in enriched primary microglia identifies key inflammatory readouts among 62 analytes.

A



1 : IL-6 3: IL12-p40/p70 5: TNF- α
 2: MCP-5/CCL-12 4: IL-1 β 6: CCL-5/RANTES

B



Supplement Fig 4. Comparison of cytokine responses between enriched microglia and mixed glia reveals shared trends.

